Study of the Electrochemical Corrosion Behaviour of X70 Steel in H_2SO_4 Contaminated Silty Soil

Peng Han, Pengju Han[*], Ruizhen Xie, Bin He, Xiaohong Bai

Department of Civil Engineering, Taiyuan University of Technology, Taiyuan 030024, P. R. China
[*]E-mail: 13834569544@163.com

In this paper, electrochemical impedance spectroscopy (EIS), polarization curves (PC), scanning electron microscopy (SEM), and energy dispersive spectroscopy (EDS) were used to test the electrochemical corrosion behaviour of X70 steel in contaminated silty soil with different pH values under indoor simulation conditions. Four different pH values of contaminated silty soil (1.50, 3.78, 5.03 and 7.07) were obtained through different concentrations of H_2SO_4 solution. The experimental results show that silty soil contaminated with H_2SO_4 solution accelerated the corrosion rate of X70 steel. In addition, the corrosion rate increased with a decrease in the pH values of the contaminated silty soil. However, the corrosion rate decreased with an increase in corrosion time due to an accumulation of corrosion products on the X70 steel surface. In weakly acidic contaminated silty soil and neutral silty soil (pH=7.07 and 5.03), the corrosion morphology and corrosion type of X70 steel are similar, i.e., a large number of silty soil particles and deep reddish-brown corrosion products (iron oxides) were evenly covered on the X70 steel sample. Additionally, the corrosion of the sample was relatively slight after removing the cover layer, and the corrosion pits were shallow and small and evenly distributed on the surface of the X70 steel. However, in strongly acidic (pH=1.50, 3.78) contaminated silty soil, the X70 steel was seriously corroded. Among the contaminated silty soil with a pH of 3.78, a large amount of dark red-brown rust was generated on the X70 steel surface. Large-sized corrosion pits and grooves were evident after derusting. When the pH reached 1.50, two-thirds of the surface of the X70 steel were covered by a layer of milky-yellow corrosion products (sulfur-containing compounds), which protected it from corrosion. However, the area that was not significantly covered was seriously corroded, and a large number of deep and large pits appeared on the X70 steel surface.

1. INTRODUCTION

With an increase in industrialization in China, the demand for oil, natural gas and other resources is becoming increasingly urgent in various regions. However, the distribution of resources in China is not directly proportional to the population density. The distribution of resources has greatly

failed to meet the needs of individuals. In view of this uneven distribution of energy and the population, increasingly applications of long-distance and long-span buried pipeline steel have been used for the transportation of oil and natural gas[1], such as "West-East Gas Transmission"[2]. These pipelines have not only greatly eased the pressure on railway transportation but also ensured the safe and rapid supply of resources such as oil and natural gas. However, the rapid economic development in China has increased the number of serious environmental pollution problems. For example, type of sulfuric acid rain often occurs in central and eastern China due to the excessive emission of automobile exhaust gas and the burning of coal with a high sulfur content. Acid rain is very harmful and will reduce the soil pH and change the soil corrosiveness. These issues may exacerbate the corrosion of stressed steel in some underground reinforced concrete buildings or structures[3], leading to a significant weakening of their mechanical properties, which may cause safety hazards in buildings. Similarly, contaminated soil may also aggravate the corrosion of buried pipeline steel, which may cause partial leakage in some areas[4]. In recent years, environmental pollution and economic losses caused by the leakage of underground pipeline steel cannot be ignored.

Many scholars had studied the mechanism of metal corrosion, especially buried pipeline steel. Currently, type of buried steel used include X52, X60, X70, X80 and Q235, whose corrosion resistance vary greatly in soil[5-10]. Considering the factors of cost, corrosion resistance and strength, X70 steel is the most widely steel used in buried pipelines. At present, most of the research on the corrosion of buried pipeline steel has introduced corrosive ions into a solution or used a soil simulated solution as the corrosive medium[11-17]. However, there are still some significant differences between the soil medium and the solution medium. Therefore, increasingly more scholars have begun to explore the corrosion characteristics of steel in soil[18]. Various methods have been used in the process of analysis because of the diversity and complexity of soil, such as electrochemical impedance testing, polarization curves, electrical resistance sensors, weightlessness, electrochemical noise and other testing methods[19-27]. Nevertheless, the methods for corrosion test and analysis are not yet systematic in the soil medium. In recent years, the methods which combined scanning electron microscopy (SEM), electrochemical impedance spectroscopy (EIS), polarization curves (PC) and energy dispersive spectroscopy (EDS) were being used to study the corrosion behaviour of steel in the soil, i.e., the above methods were mainly used to study the corrosion behaviour of Q235 steel in heavy metal contaminated sandy soil[28, 31] and the corrosion characteristics of X70 steel in sandy soil with different particle sizes[33, 34]. In this paper, the corrosive medium was silty soil which widely distributed in China, and was one of the most common types of soil. Properties of silty soil were between sand and cohesive soil. Silty soil and sandy soil which mentioned above had great differences in the corrosion characteristics of the steel structure. This paper focused on the hot issues such as environmental pollution. Silty soil contaminated with different concentrations H_2SO_4 solutions were used to simulate the silty soil contaminated by acid rain and waste liquid from a suiphuric acid plant. And the paper is trying to explore the corrosion behavior of steel in different level of H_2SO_4 contaminated silty soil and providing a reference for the corrosion of buried pipeline steel and underground steel structure.

2. EXPERIMENTAL PROCEDURE

2.1 Experimental materials and pretreatment

X70 steel has been widely used for buried pipelines in China, and the main chemical composition and content of X70 steel are listed in Table 1[28]. The size of the X70 steel was 12 mm×12 mm×2 mm. The steel sample was then cleaned with alcohol. X70 steel was sanded by using different sandpapers ([#]360, [#]400, [#]800, [#]1000, [#]1200, [#]1500 and [#]2000) until there was no obvious scratches on the surface. Next, the steel was washed with deionized water and air dried. A certain length of copper wire was attached to the non-working surface of the X70 steel by a tin foil. Then, the steel was sealed with epoxy resin, leaving a 1.0 cm×1.0 cm area of the corrosive surface. Finally, the impurities on the corroded surface were cleaned with ethanol or acetone, air dried and bagged for testing.

The soil samples used in this test were silty soil, which is widely distributed in China. The soil was taken from a construction site in Shanxi province of China and was filtered through a 2.5 mm sieves. The particle analysis result is shown in Table 2. The uniformity coefficient of the soil sample was 3.78, and the coefficient of curvature was 1.58. The specific gravity of the solid particles was 2.69, the liquid limit W_L was 23.9%, the plastic limit W_P was 17.8%, and the plasticity index was 6.1. According to national standard specification, the soil sample was judged as silty soil.

Table 1. Chemical composition of X70 steel (wt.%)

C	Cr	Si	Mn	P	Ni	Mo	Cu	Co	V	S	Fe
0.07	0.02	0.21	1.91	0.01	0.02	0.23	0.01	0.01	0.01	<0.0005	Bal

Table 2. Particle analysis results

Particle size (mm)	2.25-0.075	0.075-0.05	0.05-0.01	0.01-0.005	<0.005
Content (%)	29	33.8	30.5	2.6	4.1

Contaminated silty soil with different pH values mentioned in this article was obtained by mixing dried silty soil and different masses of sulfuric acid solution, and the solutions were stirred by manual mixing to facilitate uniformity.

Table 3. Mix proportion contaminated silty soil with different pH values

Silty soil (g)	300	300	300	300
H_2SO_4 (g)	48	12	5.33	0
Water (g)	48	48	48	48
pH	1.50	3.78	5.03	7.07

The selection of the moisture content for the contaminated silty soil in this experiment is based on the results of the compaction test (the optimum moisture content is 16%). Four sets of contaminated silty soil with different pH values were obtained by controlling the mass of sulfuric acid incorporation. In addition, the pH values were tested using the PHS-3C acidity metre (LeiCi of ShangHai. China) according to the "Soil Test Method Standard" (GB_T50123-1999). The ratios of the substances are shown in Table 3. Here, water contained in the sulfuric acid was ignored (the mass fraction is 98%).

Contaminated silty soil was put into a waterproof breathable membrane for 24 hours. Four groups of contaminated silty soil were placed in a sample mould with a size of 7.07 cm×7.07 cm×7.07 cm. In addition, the height of soil was pressed into the same position. Furthermore, the prepared X70 steel was also inserted into the same position of the contaminated silty soil with different pH values and the specimens were wrapped with a waterproof and breathable membrane (Fig. 1). Corrosion behaviour of X70 steel in the specimens was tested respectively when the immerse time was up to 1 day and 14 day.

2.2 Test and characterization

The CS350 electrochemical workstation (Wuhan Corrtest Instruments) was used to acquire the PC and the EIS data of X70 steel in contaminated silty soil for 1 d and 14 d via a three-electrode system. Three test electrodes are the working electrode WR (X70 steel), the auxiliary electrode CE (platinum electrode), and the reference electrode RE (saturated calomel electrode). The schematic diagram of the experimental device is shown in Fig. 1. During the test, the temperature and humidity were controlled at 20±5 °C and a 45%±5% RH respectively. The test frequency range of EIS was 10^{-2}~10^{5} Hz. The AC sinusoidal excitation signal amplitude was 5 mV. The measurements were performed at the self-corrosion potential, and the PC scan rate was 0.167 mV/s.
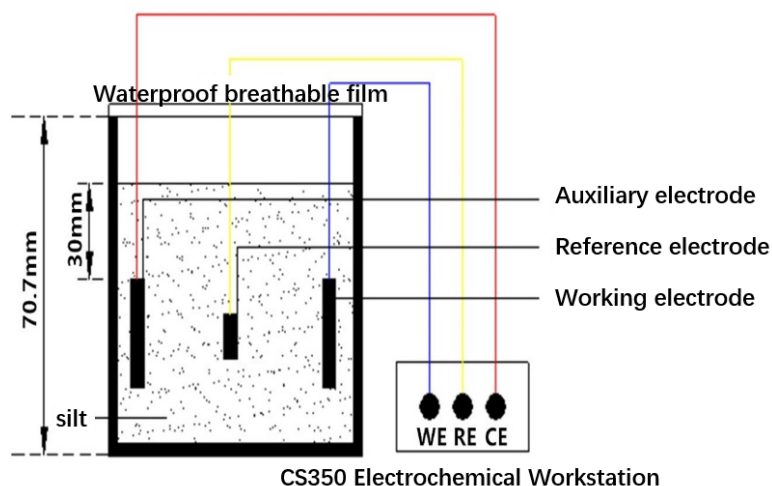
Figure 1. The schematic diagram of the system designed for the corrosion of X70 steel

After the corrosion was carried out for 14 days, the macroscopic corrosion morphology of the X70 steel was collected by a digital camera (Canon 6D SLR). The microscopic corrosion morphology of X70 steel before and after rust removal was obtained by scanning electron microscopy (SEM, TM3000) at different magnifications (100× and 500×). The corrosion products were analysed by energy dispersive spectroscopy (EDS).

3. RESULTS AND DISCUSSION

3.1 Macrocorrosion morphology

Fig. 2 shows the macroscopic corrosion morphologies of X70 steel in the contaminated silty soil with different pH values after 14 days. In different contaminated silty soil, the corrosion morphology of X70 steel was quite different. With a decrease in the pH values of the contaminated silty soil, the corrosion degree of X70 steel became increasingly serious. In contaminated silty soil with the pH values of 7.07 and 5.03, dark red-brown rust and a large amount of silty particles were found on the surface of the X70 steel. This finding may be because the silty particles are finer and more evenly distributed on the X70 steel surface during the corrosion process. In addition, oxygen was dissolved in the liquid phase part of the silty soil media. The oxygen depolarization reaction and dissolution of iron occurred together on the electrode surface. Under the effect of concentration, a kind of adhesive compound was formed, which made the silty particles firmly adhere to the surface of the X70 steel. However, characteristics of macroscopic corrosion morphology were different in strongly acidic contaminated silty soil environments (1.50 and 3.78). A large amount of hydrogen ions were contained in the liquid phase part of the silty soil media. Cathode reaction evolves from oxygen depolarization to hydrogen evolution corrosion. When the pH value was 3.78, there was no obvious adhesion of the silty particles on the surface of the X70 steel, and a large amount of deep reddish-brown rust covered the corroded surface. The uncovered areas became rough, and the metallic lustre was dull. When the pH reached 1.50, the acidity of the silty soil was further increased; two-thirds of the steel surface was covered with a layer of milky-yellow corrosion products, while the uncovered area was dark red-brown.
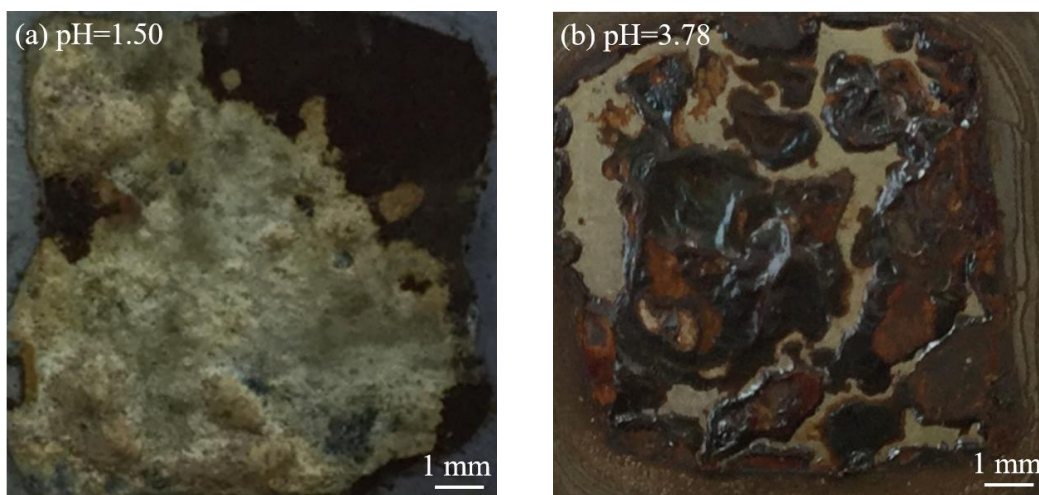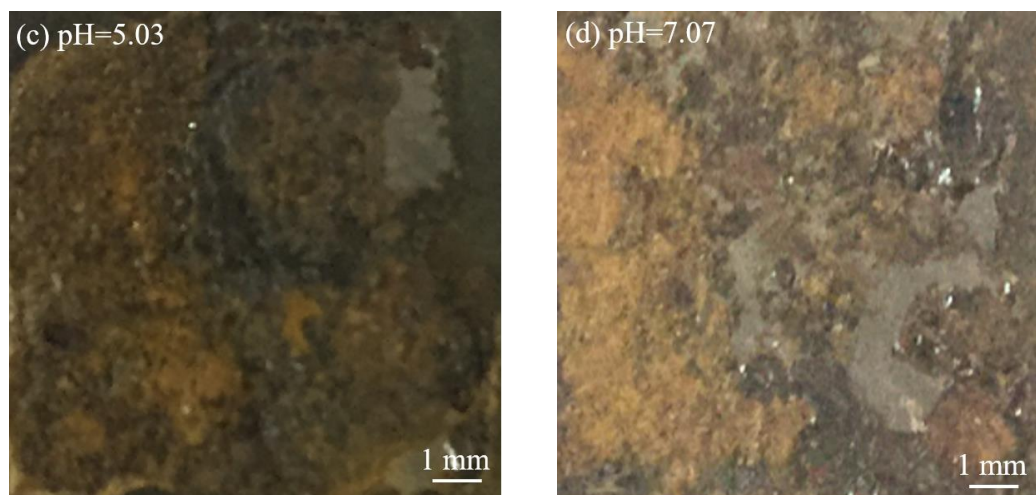
(a) pH=1.50   (b) pH=3.78

Figure 2. Macromorphology of X70 steel (14d): (a) pH=1.50; (b) pH=3.78; (c) pH=5.03; and (d) pH=7.07.

3.2 Microcorrosion morphology

As shown in Fig. 3, the representative corrosion area (before rust removal) was enlarged by 100 times to obtain the microscopic corrosion morphology. Fig. 4 shows the microscopic corrosion morphology image (after rust removal) of the X70 steel at 100 and 500 times magnifications. It can be seen that the corrosion degree, type, and the morphology of the corrosion products of the steel is significantly different.

In contaminated silty soil with a pH value of 1.50. It can be clearly seen that there were numerous fine cracks on the surface of the corrosion products, which may be caused by the continuous generation of new corrosion products and hydrogen released from a cathode reaction, leading to a certain expansion force on the surface of corrosion products. Therefore, the cracks in the surface of corrosion products appeared. However, according to the microscopic corrosion morphology (Fig. 4(a)) after derusting of the area covered by products, X70 steel was only slightly corroded. The corrosion type is mainly pitting corrosion, and the pits are shallow and small and evenly distributed on the surface of the X70 steel. The above results show that the product layers had a strong protective effect on the steel, whereas the areas that were not obviously covered by the corrosion product layer corroded seriously. Although pitting corrosion was also dominant on the surface of the steel, the pits increased both in depth and size. This increase may lead to pitting penetration of the pipeline steel in an actual project and cause leakage accidents. When the pH was 3.78, the corrosion products on the surface of the steel were loose stratification and were unevenly distributed on the X70 steel surface. It can be seen that the degree of corrosion was serious after derusting, and porphyritic corrosion pits and even corrosion gullies were found on the surface of the steel. The boundary between the pits and the outer surface of pits were obvious and showed a sharp jagged appearance. In the contaminated silty soil with the pH values of 5.03 and 7.07, the morphology of the corrosion products and type of corrosion were similar at the surface of the X70 steel.
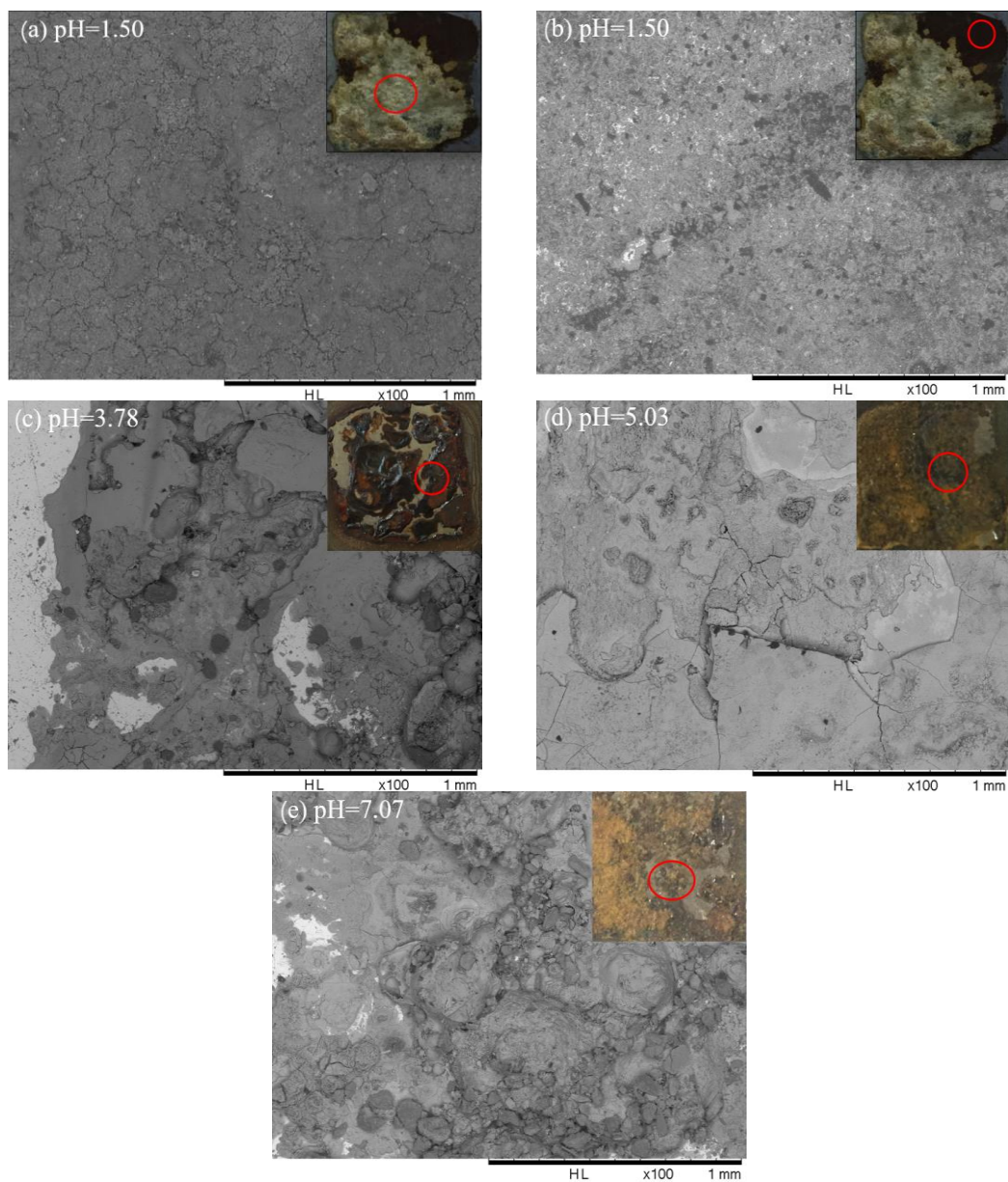
Figure 3. Micromorphology of X70 steel (before cleaning the rust): (a, b) pH=1.50; (c) pH=3.78; (d) pH=5.03; and (e) pH=7.07.
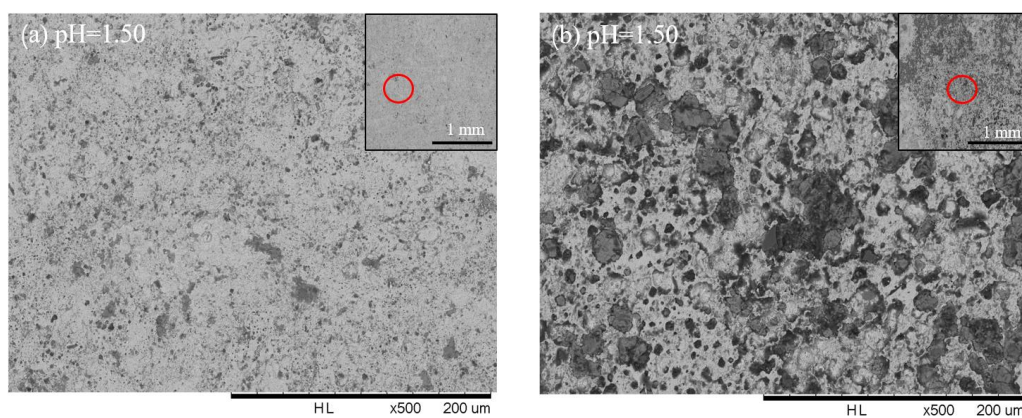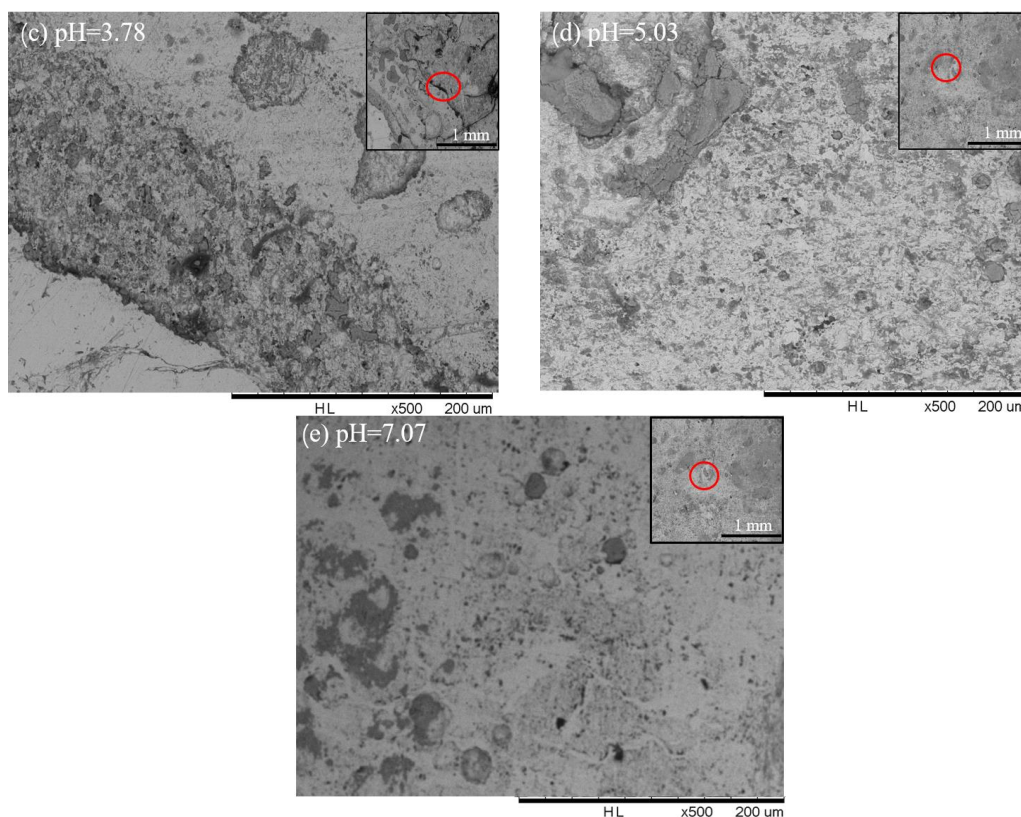
Figure 4. Micromorphology of X70 steel (after cleaning the rust): (a, b) pH=1.50; (c) pH=3.78; (d) pH=5.03; and (e) pH=7.07.

Corrosion products evenly adhered silty particles covered on the surface of the steel, and the protective effects on the steel were obvious. After rust removal, the size of the corrosion pits distributed on the surface of the steel was small and shallow, and the corrosion was relatively slight.

In summary, X70 steel was seriously corroded in the contaminated silty soil at a pH value of 3.78. In addition, at a pH of 1.50 and without a significant corrosion product layer, the steel area was also seriously corroded. When the buried pipeline steel was in the above two contaminated silty soil, corrosion damage such as pitting penetration or declining bearing capacity may occur. At pH values of 5.03 and 7.07 in silty soil environments, the corrosion of X70 steel was relatively slight. The size and depth of the corrosion pits were small and shallow. The reason for the above differences in corrosion process may be because the depolarization reaction of oxygen occurred mainly in the cathode of the X70 steel in the environment of non-contaminated silty soil (pH=7.07) or weakly acidic contaminated silty soil (pH=5.03). However, the solubility of oxygen in the liquid phase of the silty soil was relatively low; thus, it cannot provide sufficient oxygen for the corrosion processes. When the pH values reached 3.78 and 1.50, the acidity of the contaminated silty soil was strong and can provide enough hydrogen ions for the hydrogen evolution reaction of the cathode. Therefore, corrosion processes of X70 steel were fast[29, 30].

3.3 Results of EDS

As shown in Fig. 5, the EDS of the corrosion products on the X70 steel surface was collected using an energy spectrum analyser supported by a scanning electron microscope (TM3000), and the elemental type and contents of the surface corrosion products were obtained.

In contaminated silty soil at four different pH values, the type of major elements in the corrosion products on the X70 steel surface differ only slightly. Generally, Fe, O, and Si accounts for the largest proportion of elements. Fig. 5 (a, b) show the results of the energy spectrum analyses of different corrosion areas of X70 steel in contaminated silty soil at a pH value of 1.50. In areas where there was no obvious cover layer, the EDS results indicate mainly Fe and O elements. It can be inferred that the corrosion products mainly consist of iron oxides. In the milky-yellow cover layer, the Fe proportion is relatively small, and the S content is greater than the Fe content. It can be inferred that in this strongly acidic contaminated silty soil, the surface of the steel was covered by a dense layer comprising the sulfur and iron compounds, which largely protected the steel from corroding. In other contaminated silty soil environments (pH=3.78, 5.03, and 7.07), the major elements and the mass fraction of the corrosion products were not much different, i.e., the corrosion products consisted of iron oxides.
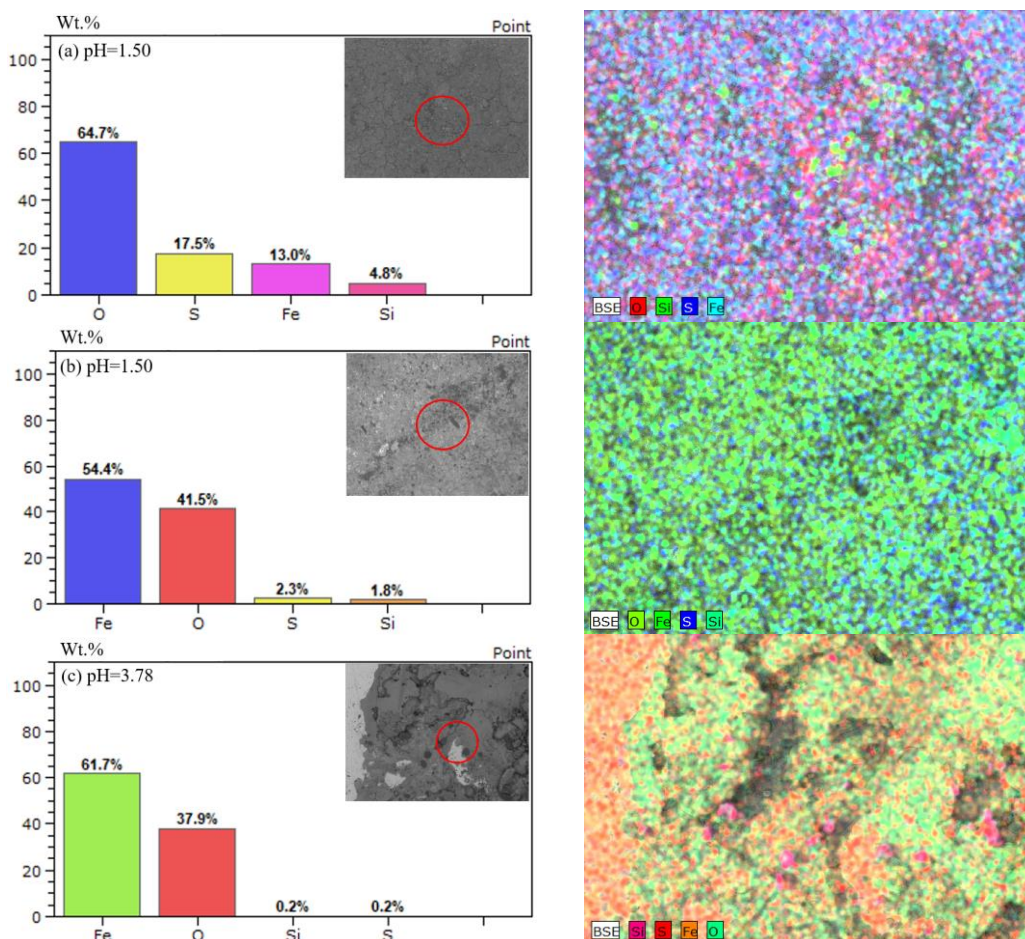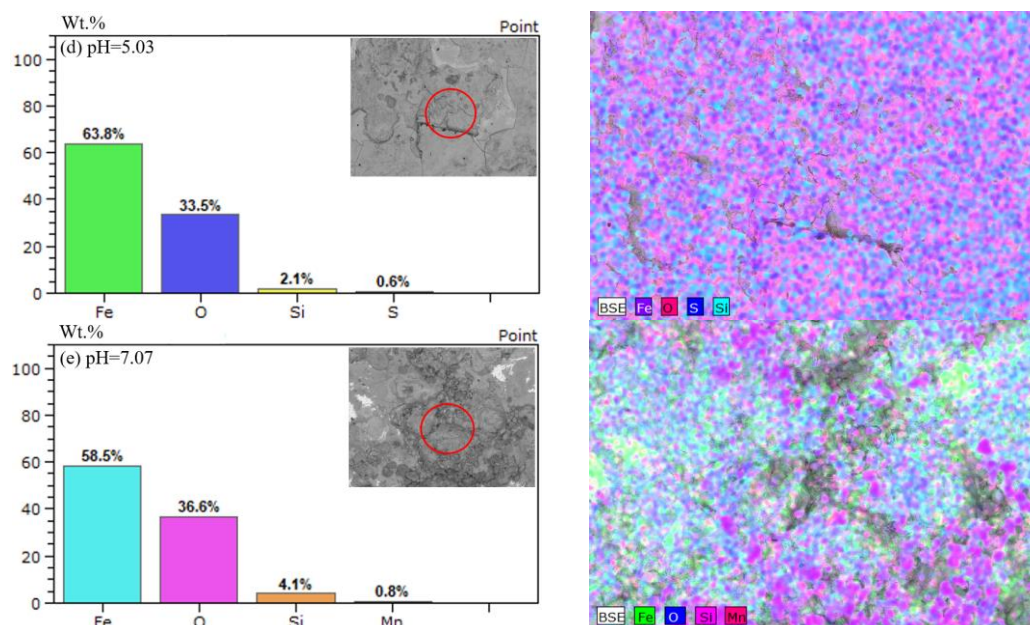
Figure 5. Element mass percentages on the X70 steel surface in contaminated silty soil at different pH values: (a, b) pH=1.50; (c) pH=3.78; (d) pH=5.03; and (e) pH=7.07.

3.4 Polarization curve analysis

Fig. 6 shows the polarization curves of X70 steel corroded in contaminated silty soil at different pH values for 1 d and 14 d. It can be seen from the Fig. 6 (a) that, except for the pH value of 1.50, the polarization curves of the anode and cathode branches were smooth; this means that no passivation film appeared or no large changes occurred on the surface of the electrode during the corrosion processes[31]. In the contaminated silty soil environment at a pH value of 1.50, a significant inflection point appeared in the anode region of the polarization curves. Combined with the previous analysis, this inflection point may be due to the strong oxidizing properties of contaminated silty soil. In addition, most of the area of the X70 steel was gradually covered by the layer of milky-yellow sulfur-iron compounds. These results suggest that large changes occurred in the region of the anode, which was reflected by the obvious inflection point in the region of the anode in the polarization curves. At the same time, the self-corrosion potentials of the polarization curves are quite different in contaminated silty soil with different pH values, especially at a pH value of 1.50. Corrosion resistance is proportional to the self-corrosion potential only when significant passivation occurs during metal corrosion. Otherwise there is no direct relationship between them [32]. It can be seen from the Fig. 6 that the polarization curves of X70 steel did not show obvious passivation at the four different pH values of the contaminated silty soil. In contaminated silty soil with a pH value of 1.50, the anodic dissolution of Fe^{2+} cannot diffuse into the liquid phase of the silty soil due to the reason that the anode surface was partially covered by corrosion products. In addition, the anodic region accumulated a large amount of Fe^{2+}, which led to an increase in the self-corrosion potential.

According to Faraday's law, the corrosion current density is proportional to the corrosion rate. With an increase in the pH values, the anode branch of the polarization curves gradually shifted to the

left, and the corrosion current density decreased in the polarization curves of X70 steel in different contaminated silty soil environments. It can be inferred that the corrosion rate of X70 steel decreased with an increase in pH values.
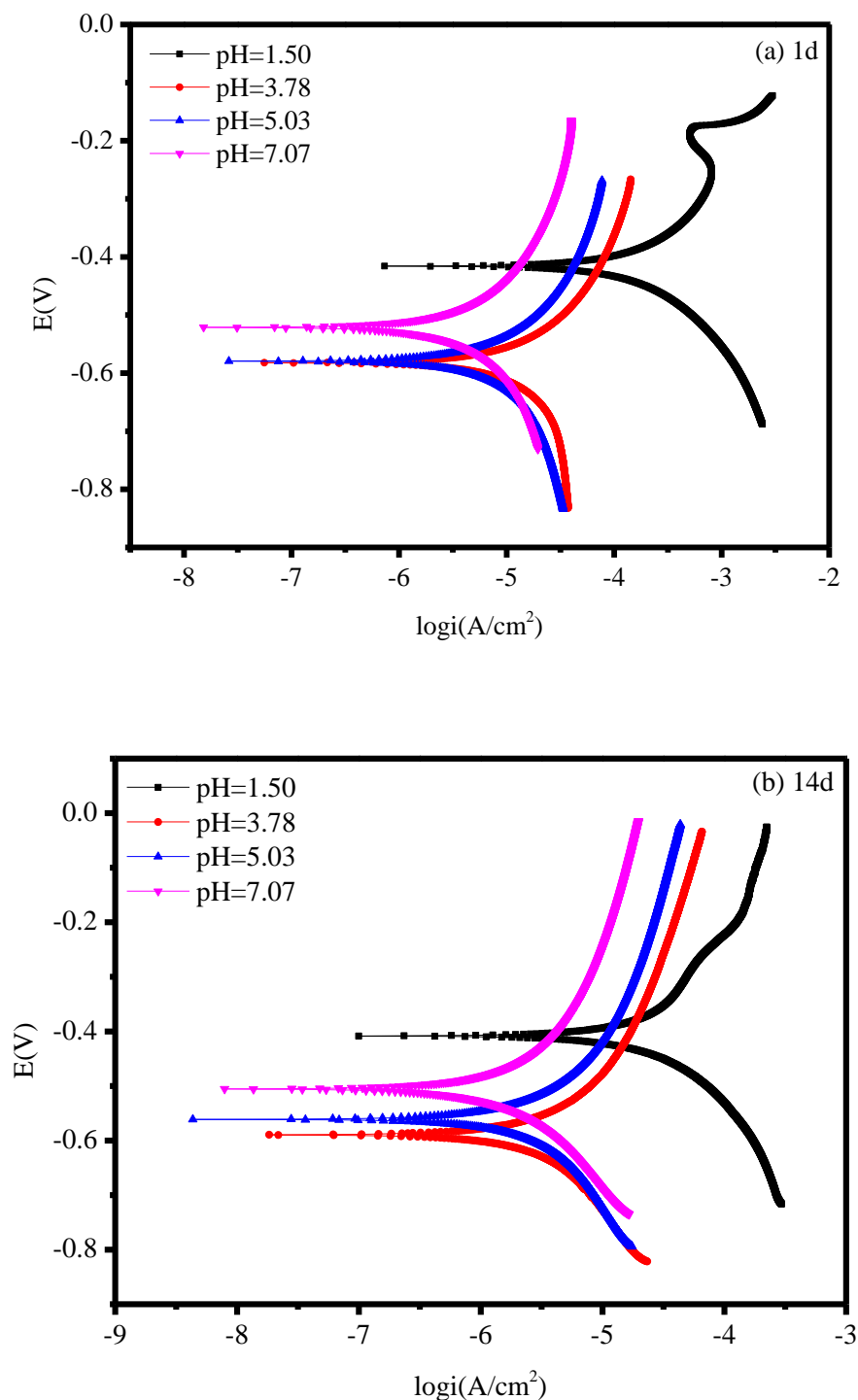
Figure 6. Polarization curves of X70 steel in the contaminated silt system at different pH values of 1.50, 3.78, 5.03 and 7.07 (1d and 14d).

To quantitatively study the PCs of X70 steel in contaminated silty soil with different pH values, the PCs were fitted by Tafel extrapolation methods using CVIEW software to obtain the corrosion potential E_{corr}, the self-corrosion current density I_{corr}, and the Tafel slopes of the anode and cathode, b_a and b_c, respectively. The fitting parameters were listed in Table 4. From Table 4, it can be seen that in contaminated silty soil with a pH value of 1.50, the corrosion potential reached a maximum of -416 mV. When corrosion time reached 14 d, the corrosion potential slightly increased to -4090 mV. The self-corrosion current density decreased with an increase in the pH values, and the maximum current density was 451 $\mu A/cm^2$ for 1 d. When the corrosion was carried out to 14 d, the minimum corrosion current density was 4 $\mu A/cm^2$ in the non-contaminated silty soil environment. Overall, the self-corrosion current density was reduced to 14 d relative to that at 1 d. This reduction may be due to the protection of the gradual accumulation of the corrosion products layer on the X70 steel surface, resulting in a decrease in the corrosion rate. The Tafel slopes of the cathode and anode did not show obvious rules and will not be discussed here.

Table 4. The fitting results of the X70 steel polarization curves (1 d and 14 d)

Time (day)	pH	E_{corr}, mV	I_{corr}, $\mu A/cm^2$	B_a, V/dec	$-B_c$, V/dec
	1.50	-416	451	327	419
	3.78	-582	47	1919	395
1	5.03	-579	26	983	415
	7.07	-521	11	531	384
	1.50	-409	94	2897	393
	3.78	-590	10	475	751
14	5.03	-561	8	497	603
	7.07	-506	4	572	411

3.5 EIS analysis

Fig. 7 shows the EIS spectra of X70 steel when it was corroded in contaminated silty soil at different pH values for 1 d and 14 d. From the plots, the impedance spectra are similar at various corrosion times and pH values, but the sizes are obviously different. In the non-contaminated silty soil, the impedance spectrum radius was the largest, and in the pH value of 1.50 was the smallest. In general, the impedance arc radius increased with an increase in pH in the two measured corrosive time. It can be seen that the sulfuric acid contaminated silty soil greatly influenced the corrosion processes of the X70 steel.

From EIS data, there were two time parameters in the corrosion process, namely, the capacitive reactance arc in the high and middle-low frequency regions. The capacitive arc of the high-frequency region reflects the characteristics of the corrosion product films on the electrode surface. In addition, the capacitive arc of the medium-low frequency region reflects the characteristics of the charges when they passed through the double layer. By analysing the charges of transfer resistor R_{ct} and the double-layer capacitance QPE (include QPE-Y and QPE-n), the corrosion rate and corrosion degree of the X70 steel can be judged to some extent.

Fig. 7 shows that the radius of capacitive arc in the high-frequency region decreased with an increase in the pH value. Therefore, it can be inferred that the protective effect of corrosion products film on X70 steel increased with an increase in the pH values of the contaminated silty soil. In general, the radius of the capacitive reactance arc in the middle-low frequency region shows an increasing trend with an increase in pH values. The radius of the capacitive reactance arc was the largest in the non-contaminated silty soil at a pH value of 7.07.
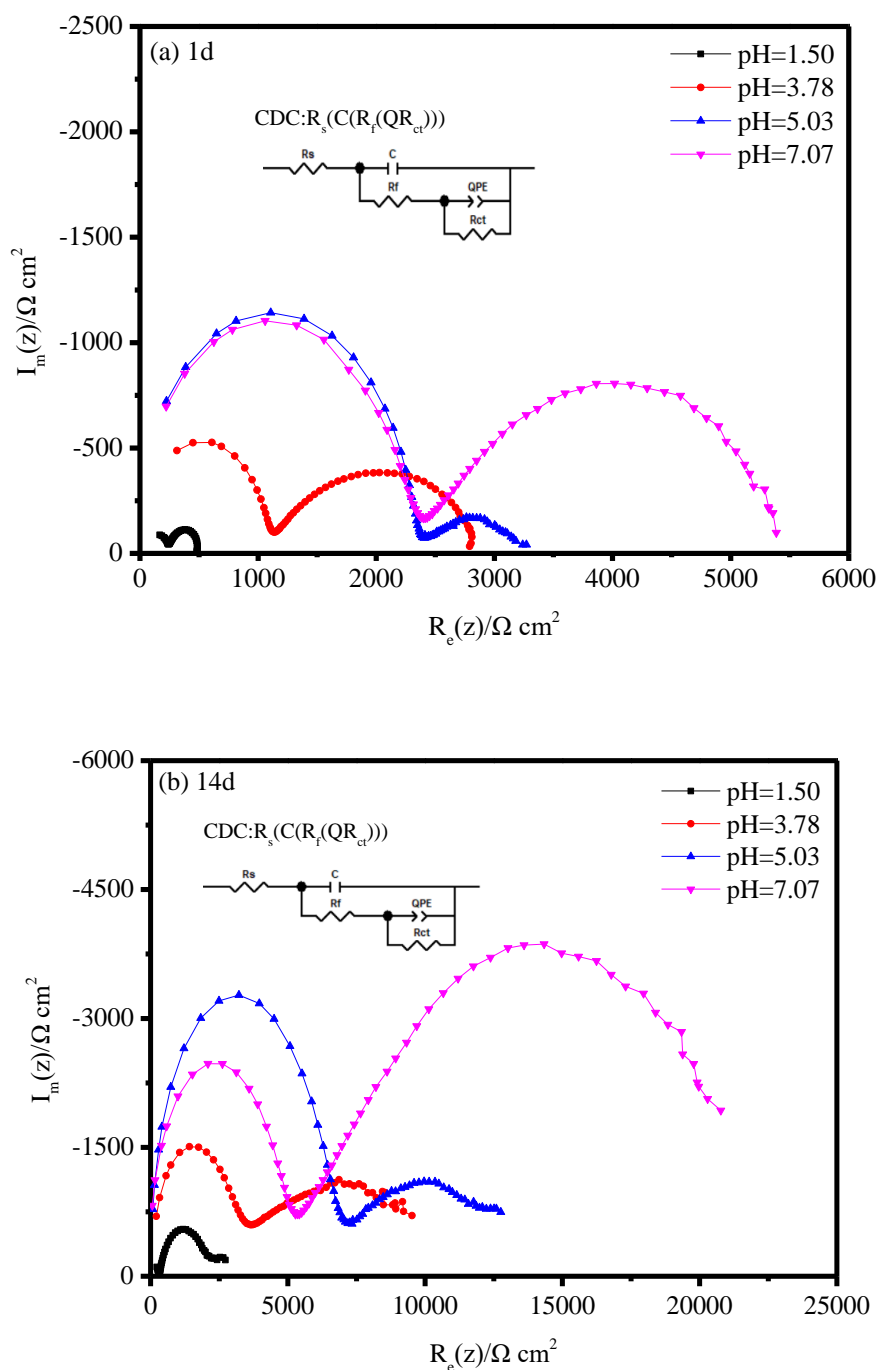
Figure 7. EIS of X70 steel in the contaminated silt system at different pH values of 1.50, 3.78, 5.03 and 7.07 (1d and 14d).

The EIS data were further analysed using the equivalent circuit R_s (C (R_f (QR_{ct}))) through ZSimwin software[33]. The illustration of the equivalent circuit is shown in Fig. 7. Each electrochemical element is defined as follows: R_s is the solution resistance, C is the corrosion product film capacitance, R_f is the resistance, QPE-Y is the double layer capacitance, QPE-n is the dispersion coefficient and R_{ct} is the charge transfer resistance[34]. The fitted electrochemical parameters are listed in Table 5. The resistance R_f of the corrosion products increased significantly with an increase in the pH value and also increased with the time of corrosion. This increase may be because the surface corrosion products of X70 steel adhere to a large amount of silty particles in the neutral and weakly acidic contaminated silty soil, leading to an increase in the corrosion product film resistance. The charges transfer resistance R_{ct} reflected the resistance of the charges across the double layer. R_{ct} is positively related to the reciprocal of the corrosion rate. It can be seen from Table 5 that the charge transfer resistance decreased with an increase in the pH value; this trend is the same as that reflected by the polarization curves.

Table 5. The fitting results of X70 steel EIS spectra (1 d and 14 d)

Time (day)	pH	R_s ($\Omega \cdot cm^2$)	C (F)	R_f ($\Omega \cdot cm^2$)	QPE		R_{ct} ($\Omega \cdot cm^2$)
					QPE-Y ($Sp \cdot \Omega^{-1} \cdot cm^{-2}$)	QPE-n	
1	1.50	39.91	5.70E-9	192	2.68E-5	0.69	293
	3.78	6.22	2.05E-9	1056	8.34E-5	0.50	1876
	5.03	3.41	1.82E-9	2263	4.07E-6	0.38	1091
	7.07	2.88	1.75E-9	2296	6.86E-5	0.54	3422
14	1.50	76.17	4.63E-9	221	9.98E-5	0.65	2119
	3.78	14.42	1.73E-9	2641	5.24E-5	0.31	8573
	5.03	1.36	1.61E-9	4892	5.20E-5	0.38	7290
	7.07	1.19	1.56E-9	6370	2.73E-5	0.47	18840

One anode reaction and two cathode reactions were included among the corrosion processes of X70 steel in contaminated silty soil with different pH values[35, 36]. In strongly acidic contaminated silty soil, the electrolyte in the liquid phase of the silty soil medium was adsorbed on the surface of the X70 steel. H_2O became OH^-, and then a single electron was discharged and formed the corrosion intermediate $Fe(OH)_{ad}$, which adsorbed on the X70 steel surface. Then, the $Fe(OH)_{ad}$ discharge became $FeOH^+$ and dissolved in the electrolyte solution. This process was the control step of the anodic reaction. Finally, $FeOH^+$ was converted to Fe^{2+} in the electrolyte solution. The reaction equations (1), (2) and (3) are listed as follows[32]:

$$Fe+H_2O \rightarrow Fe(OH)_{ad}+H^++e^- \qquad (1)$$
$$Fe(OH)_{ad} \rightarrow FeOH^++e^- \qquad (2)$$
$$FeOH^++H^+ \rightarrow Fe^{2+}+H_2O \qquad (3)$$
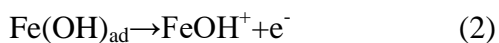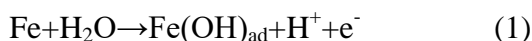
In neutral (pH=7.07) and weakly acidic (pH=5.03) contaminated silty soil, the cathodic reaction was shown in equations (4), (5) and (6) below[37, 38]:

$$O_2+e^-\rightarrow O_2^- \qquad (4)$$
$$O_2^-+H_2O+e^-\rightarrow HO_2^-+OH^-(RDS) \qquad (5)$$
$$HO_2^-+H_2O+2e^-\rightarrow 3OH^- \qquad (6)$$

In the strongly acidic (pH=1.50 and 3.78) contaminated silty soil, the cathodic reaction was shown in equations (7) and (8) below[32]:

$$H^++e^-\rightarrow H_{ad} \qquad (7)$$
$$2H_{ad}\rightarrow H_2/H^++H_{ad}+ e^-\rightarrow H_2 \qquad (8)$$
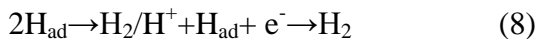
4. CONCLUSIONS

In this paper, electrochemical corrosion characteristics of X70 steel in silty soil contaminated by H_2SO_4 solution at different pH values were studied by means of electrochemical tests, SEM and EDS. The following conclusions were obtained.

(1) The corrosion morphology of X70 steel was considerably different with changes in the pH values in the contaminated silty soil. With pH values of 5.03 and 7.07, a large number of fine silty particles adhered to the surface of the X70 steel. At the same time, it can be seen that a small amount of red-brown rust was also evident on the surface. In the contaminated silty soil with a pH of 3.78, considerable red-brown rust covered the steel surface, and the surface of the area without a significant corrosion product layer was rough with a metallic lustre. When the pH value reached 1.50, the X70 steel was partially covered with a layer of milky-yellow corrosion products, while the uncovered area was dark red-brown.

(2) The corrosion types of X70 steel exhibited a great variation in contaminated silty soil with different pH values. For pH values of 5.03 and 7.07, the type of corrosion was mainly pitting corrosion, and the pits were shallow and small, and moderately distributed on the surface of the X70 steel. In the contaminated silty soil with a pH value of 3.78, porphyritic corrosion pits and corrosion grooves can be found, and their size and depth have increased. When the pH value reached 1.50, many deep pits were found on the surface of X70 steel in the area that was not covered by milky-yellow corrosion products. These deep pits can cause pitting penetration and leakage accidents in actual buried pipeline steel engineering.

(3) The corrosion process of X70 steel in contaminated silty soil is mainly controlled by electrochemical activation. The corrosion rate increased with a decrease in the pH values and decreased with the corrosion time. The corrosion product films on the surface of the X70 steel increased with an increase in pH; the protective effect of the steel was also significantly increased.

(4) The corrosion products of X70 steel were mainly iron oxide in contaminated silty soil with the different pH values. At the pH value of 1.50, the X70 steel was covered by corrosion products that contained sulfur and iron compounds.

References

1. L. Zheng, *Baosteel Technol. Res.,* 4 (2010) 36.
2. H. Li, C. Huo, L. Ji and Y. Li, *J. Iron and Steel Res. (Int),* S1 (2011) 39.
3. H. W. Song and V. Saraswathy, *Int. J. Electrochem. Sci.,* 2 (2007) 1.
4. I. Matsushima, *Bulletin of Maebashi Insti. Technol.,* 5 (2002) 83.
5. V. d. F. Cunha Lins, M. L. Magalhães Ferreira and P. A. Saliba, *J. Mat. Res. Technol.,* 1 (2012) 161.
6. E. A. Noor and A. H. Al-Moubaraki, *Arabian J. Sci. Eng.,* 39 (2014) 5421.
7. Y. H. Wu, T. M. Liu, C. Sun, J. Xu and C. K. Yu, *Corros. Eng. Sci. Technol.,* 45 (2013) 136.
8. C. M. Yan, S. C, X. J, K. W and J. N. Murray, *Int. J. Electrochem. Sci.,* 10 (2015) 1762.
9. S. S. Xin and M. C. Li, *Corros. Sci.,* 81 (2014) 96.
10. S. Marcelin, N. Pébère and S. Régnier, *Electrochem. Acta,* 87 (2013) 32.
11. T. M. Liu, Y. H. Wu, S. X. Luo and C. Sun, *Materialwiss Werkst,* 41 (2010) 228.
12. P. VEP and A. A, *Corros.,* 68 (2012) 035005.
13. L. P, D. CW, L. XG and L. Z, *Int. J. Min. Met. Mater.,* 16 (2009) 407.
14. M. Jeannin, D. Calonnec, R. Sabot and P. Refait, *Corros. Sci.,* 52 (2010) 2026.
15. X. Chen, C. W. Du, X. G. Li, C. He and P. Liang, *Int. J. Min. Met. Mater.,* 16 (2009) 525.
16. E. A. Noor and A. H. Al-Moubaraki, *Int. J. Electrochem. Sci.,* 3 (2008) 806.
17. A. S. Hamdy, E. El-Shenawy and T. El-Bitar, *Int. J. Electrochem. Sci.,* 1 (2006) 171.
18. O. A. Oyewole, *Corros. Sci.,* 5 (2011) 1.
19. L. J. Zhang, Z. Zhang, F. H. Cao, J. Q. Zhang, J. M. Wang and C. N. Cao, *Acta Metall. Sin-engl.,* 17(2004) 907.
20. N. Naing Aung and Y. -J. Tan, *Corros. Sci.,* 46 (2004) 3057.
21. S. Wang, D. Liu, N. Du, Q. Zhao and J. Xiao, *Adv. Mater. Sci. Eng.,* 2015 (2015) 1.
22. A. Legat, *Electrochem. Acta,* 52 (2007) 7590.
23. S. Li, Y. -G. Kim, S. Jung, H. -S. Song and S. -M. Lee, Sensor. Actust. B-Chem., 120 (2007) 368.
24. S. Li, S. Jung, K. -w. Park, S. -M. Lee and Y. -G. Kim, Mater. Chem. Phys., 103 (2007) 9.
25. J. Y. Huang, Y. B. Qiu and X. P. Guo, *Mater. Corros.,* 60 (2009) 527.
26. M. M and R. P, *Br. Corros. J.,* 20 (1985) 117.
27. O. Farghaly, R. Hameed and A. Abu-Nawwas, *Int. J. Electrochem. Sci.,* 9 (2014) 3287.
28. P. J. Han. *Int. J. Electrochem. Sci.,* 12 (2017) 7668.
29. X. Mao, X. Liu and R. W. Revie, *Corros.,* 50 (1994) 651.
30. Z. Y. Liu, X. G. Li and Y. F. Cheng, *Electrochem. Acta,* 60 (2012) 259.
31. P. J. Han, *Int. J. Electrochem. Sci.,* 11 (2016) 9491.
32. C. N. Cao, Principles of Electrochemistry of corrosion, Beijing Industrial Press (2008) Beijing, China.
33. B. He, P. J. Han, L. Hou, D. C. Zhang and X.H. Bai, *Eng. Fail. Anal.,* 80 (2017) 325.
34. B. He, P. J. Han, C. Lu and X. H. Bai, *Eng. Fail. Anal.,* 58 (2015) 19.
35. S. Zhang, *Int. J. Electrochem. Sci.,* 13 (2018) 3246.
36. B. Yuan, *Int. J. Electrochem. Sci.,* 13 (2018) 3396.
37. A. P. Yadav, A. Nishikata, T. Tsuru, *J. Electroanal. Chem.*, 585 (2005) 142.
38. H. Dafydd, D. A. Worsley, H. N. McMurray, *Corros. Sci.*, 47 (2005) 3006.